Development 125, 621-634 (1998)
Printed in Great Britain © The Company of Biologists Limited 1998
DEV9579

Inner ear and maternal reproductive defects in mice lacking the *Hmx3* homeobox gene

Weidong Wang[1], Thomas Van De Water[2] and Thomas Lufkin[1,*]

[1]Brookdale Center for Developmental and Molecular Biology, Mount Sinai School of Medicine, One Gustave L. Levy Place, New York, NY 10029-6574, USA
[2]Departments of Otoryngology and Neuroscience, Albert Einstein College of Medicine, 1300 Morris Park Avenue, Bronx, NY 10461, USA
*Author for correspondence (e-mail: Lufkit01@doc.mssm.edu)

Accepted 21 November 1997: published on WWW 22 January 1998

SUMMARY

The *Hmx* homeobox gene family is of ancient origin, being present in species as diverse as *Drosophila*, sea urchin and mammals. The three members of the murine *Hmx* family, designated *Hmx1*, *Hmx2* and *Hmx3*, are expressed in tissues that suggest a common functional role in sensory organ development and pregnancy. *Hmx3* is one of the earliest markers for vestibular inner ear development during embryogenesis, and is also upregulated in the myometrium of the uterus during pregnancy. Targeted disruption of the *Hmx3* gene results in mice with abnormal circling behavior and severe vestibular defects owing to a depletion of sensory cells in the saccule and utricle, and a complete loss of the horizontal semicircular canal crista, as well as a fusion of the utricle and saccule endolymphatic spaces into a common utriculosaccular cavity. Both the sensory and secretory epithelium of the cochlear duct appear normal in the *Hmx3* null animals. The majority of *Hmx3* null females have a reproductive defect. *Hmx3* null females can be fertilized and their embryos undergo normal preimplantation development, but the embryos fail to implant successfully in the *Hmx3* null uterus and subsequently die. Transfer of preimplantation embryos from mutant *Hmx3* uterine horns to wild-type pseudopregnant females results in successful pregnancy, indicating a failure of the *Hmx3* null uterus to support normal post-implantation pregnancy. Molecular analysis revealed the perturbation of *Hmx*, *Wnt* and LIF gene expression in the *Hmx3* null uterus. Interestingly, expression of both *Hmx1* and *Hmx2* is downregulated in the *Hmx3* null uterus, suggesting a hierarchical relationship among the three *Hmx* genes during pregnancy.

Key words: Homeobox gene, Inner ear, Pregnancy, Gene knockout, Mouse

INTRODUCTION

The *Hmx* homeobox gene family was first identified in humans (Stadler et al., 1992) and subsequently in a number of species ranging from *Drosophila* to higher vertebrates (Bober et al., 1994; Martinez and Davidson, 1997; Stadler et al., 1995; Stadler and Solursh, 1994; Wang et al., 1990; Yoshiura et al., 1997). While there appears to be only a single *Hmx* gene in *Drosophila*, at least three *Hmx* genes (*Hmx1*, *Hmx2* and *Hmx3*) are present in the mammalian genome (Stadler et al., 1995). The *Hmx* genes are a distinct homeobox gene family unto themselves, and are unrelated to any of the larger classes of homeobox genes (e.g. *Hox*, *NK*, *Dlx*). The gene most closely related to the *Hmx* family, based upon amino acid similarity, is the *Soho-1* homeobox gene from chick, for which there is currently only one member described (Deitcher et al., 1994). The distribution of *Hmx* transcripts during vertebrate development has been examined in a number of species, and appears to be conserved among vertebrates (Bober et al., 1994; Rinkwitz-Brandt et al., 1995; Stadler et al., 1992; Stadler and Solursh, 1994; Yoshiura et al., 1997). Overlapping expression domains for the *Hmx* genes include the first and second branchial arches, central and peripheral nervous systems, and the uterus. *Hmx2* and *Hmx3* (previously called *Nkx5.2* and *Nkx5.1*, respectively (Bober et al., 1994)) are remarkable in that both are expressed in the developing inner ear, with *Hmx2* having a slightly later onset of expression relative to *Hmx3*. *Hmx3* is unique in its expression characteristics, being one of the earliest developmental markers for inner ear development. In the mouse, *Hmx3* is expressed in the otic epithelium from the otic placode stage (E8.5) (Rinkwitz-Brandt et al., 1995, 1996) and persists in this tissue throughout gestation. By E9.5, the expression of *Hmx3* shows a gradient of expression intensity, with stronger expression localized in the rostrodorsal portion of the otic vesicle. This differential expression becomes increasing more pronounced, and by E13.5 *Hmx3* expression is almost exclusively limited to the vestibular portion of the inner ear. In adult mice, the *Hmx* genes are expressed in the uterus of unpregnant females, where expression is primarily restricted to the medial portion of the stroma. During pregnancy, *Hmx1*, *Hmx2* and *Hmx3* are strongly upregulated in the uterine myometrium. To examine the unique developmental

role of the *Hmx3* gene, we have generated a null mutation by gene targeting. Analysis of the resulting phenotype in *Hmx3* null animals indicates a critical role for *Hmx3* in inner ear vestibular development and pregnancy.

MATERIALS AND METHODS

Library screening and *Hmx3* gene cloning and targeting constructs

A mouse 129/Sv genomic library constructed into lambda phage DashII vector was screened at low stringency conditions with the PCR-amplified human *HMX1* homeobox. Positive phage clones were then subcloned into pTZ18R (USB). To determine the identity of the cloned phage, degenerate primers, derived from the highly conserved KIWFQN sequence in the third helix of the homeodomain, were used for sequencing the homeobox regions. These degenerate primers are TL104 (5′RTTYTGRAACCADATYTT3′) and TL105 (5′AARATH-TGGTTYCARAAN3′), where R is A or G, Y is C or T, D is G, A or T, H is A, C or T and N is A, C, G or T. Sequence analysis was carried out by the dideoxy chain termination method (Sanger et al., 1977) as recommended by USB, except that 200 ng of degenerate oligo was used for each sequence reaction. Among 2×10^6 phage screened, three independent overlapping clones, which cover an approximately 24 kb genomic region, were identified to contain the mouse *Hmx3* gene. For targeting constructs, an 11.5 kb *Xba*I genomic fragment spanning the homeobox was subcloned into pTZ18R. In the resulting plasmid, the neomycin-resistance cassette (*neo*) or the IRES-*lacZ*+neomycin reporter was inserted into the unique *Xho*I site located in the *Hmx3* homeobox sequence. The targeting constructs were linearized by *Sal*I digestion for electroporation.

RNAse protection

RNAse protection was performed essentially as previously described (Lufkin et al., 1993). Total RNA from wild-type, $Hmx3^{+/-}$ and $Hmx3^{-/-}$ E11.5 stage embryos was extracted by a single-step isolation method using guanidinium thiocyanate (Chomczynski and Sacchi, 1987). 100 μg total RNA from each sample was used for RNAse protection analysis. A 472 bp PCR-amplified fragment containing the *Hmx3* homeobox region was used to make ^{32}P-labeled antisense riboprobe. This probe protects a 472 bp wild-type RNA fragment as well as two 308 bp and 164 bp RNA fragments. The internal control probe was derived from a 271 bp cDNA fragment from the mouse beta-actin gene. Hybridization was performed at 55°C. The samples were then digested with 40 μg/ml RNaseA and 2 μg/ml RNaseT1. After precipitation, the samples were run on an 8% acrylamide gel and exposed to X-OMAT film for 10 days.

ES cell culture and transgenic mouse production

ES cell transfections, chimera production and testing, and genotyping of offspring are essentially as previously described (Lufkin et al., 1991, 1993). Both R1 and D3 ES cells (Gossler et al., 1986; Nagy et al., 1990; Nagy and Rossant, 1993) were used for electroporation and chimera production with equivalent success. Positive ES cell lines were microinjected into C57BL/6J blastocysts and resulting male chimeras were backcrossed to either C57BL/6J females for a mixed genetic background, or to 129/Sv females for an isogenic background. $Hmx3^{lacZ}$ heterozygotes were generated by the Tetraploid↔ES cell aggregation technique essentially as described (Nagy et al., 1990; Nagy and Rossant, 1993), using CD-1 mice to produce tetraploid embryos. Blastomere fusion was carried out using a BLS CF-150 Cell-fusion apparatus and a GPT-250 electrode chamber in 0.3 M Mannitol (Sigma). Fused embryos were transferred to a microdrop of KSOM (Specialty Media) and incubated overnight to the 2-cell or 4-cell stage. The zona pellucida was subsequently removed with Tyrode's Solution and aggregates were set up with 2-4 tetraploid embryos per ES cell clump in a microdepression in KSOM under oil at 37°C and 5% CO_2. 24-48 hours later, the resulting expanded chimeric embryos were reimplanted into E2.5 Swiss-Webster pseudopregnant females. Embryo collection and β-galactosidase staining of embryos were performed as previously described (Frasch et al., 1995).

RNA in situ hybridization

Embryo tissues were fixed in 4% paraformaldehyde overnight, washed in PBS, and for section preparations, dehydrated through graded ethanols, followed by two changes of Americlear (Fisher) and embedded in Paraplast (Fisher) overnight under vacuum. Sections of 6-8 μm were cut and floated onto Plus+ slides (Fisher), dried and stored at 4°C. [^{35}S] probes were synthesized using either T3, T7 and SP6 polymerase according to the manufacturers' specifications (New England Biolabs, Stratagene). Antisense RNA probe was prepared and employed essentially as described (Tribioli et al., 1997; Wang et al., 1996). Following hybridization and washing, the sections were air dried and exposed overnight to film to determine signal strength. Autoradiography was performed by dipping the slides in a 1:3 ration of H_2O:Kodak NBT2 emulsion, air drying and exposing for 3-7 days. This was followed by developing in Kodak D19 and hematoxylin counterstaining.

The RNA in situ probe for *Hmx1* is derived from the 3′UTR of the *Hmx1* cDNA (Yoshiura et al., 1997). The 256 bp *Xho*I-*Bam*HI fragment was subcloned into the vector pT7T3a (Pharmacia) resulting in plasmid pT7T3a-19. The antisense probe was transcribed from the *Xho*I-linearized pT7T3a-19 with T7 RNA polymerase. The sense probe was generated by transcription of *Bam*HI-linearized pT7T3a-19 with T3 RNA polymerase. The *Hmx2* in situ probe was produced from plasmid pW187. An 1.2 kb *Xho*I genomic fragment containing the 3′ portion of the *Hmx2* gene was subcloned into pBluescriptKS$^+$ generating pW51a. pW187 was derived from pW51a by deleting the 340 bp *Xho*I-*Hin*dIII fragment, which contains the 3′ portion of the *Hmx2* homeobox. The resulting pW187 contains the entire *Hmx2* 3′UTR. Antisense probe for *Hmx2* was generated by the transcription of *Hin*dIII-linearized pW187 with T3 RNA polymerase. The sense probe was transcribed from *Xho*I-linearized pW187 with T7 RNA polymerase. For *Hmx3*, pW186 was generated by subcloning a 604 bp *Bgl*II genomic fragment of the *Hmx3* gene into vector pBluescriptKS$^+$. This genomic fragment contains the second exon of the *Hmx3* gene. The antisense probe was made by transcription of the *Eco*RI-linearized pW186 with T7 RNA polymerase. The sense probe was transcribed from the *Xho*I-linearized pW186 with T3 RNA polymerase. The probe for *Wnt7A* was derived from plasmid p567 (from Andrew McMahon). This plasmid contains a 400 bp insert, which spans the position of 1189-1589 bp of the *Wnt7A* cDNA (Parr and McMahon, 1995). The *Wnt4* probe was transcribed from plasmid p405. The insert covers the region from 851 to 1275 bp of the *Wnt4* cDNA (Stark et al., 1994). The *Wnt5A* in situ probe was transcribed from plasmid p59, where the insert is a 400 bp PCR-amplified fragment of mouse *Wnt5A* gene, which encodes the region from amino acids 260 to 391 of the Wnt5A protein (Gavin et al., 1990). A 387 bp fragment of the mouse smooth muscle myosin heavy chain cDNA, which contains exon I (75 nucleotide of the untranslated sequence) and most of exon II (remaining 5′UTR plus about 295 bp of coding region), was used as a template to make RNA in situ probe (Miano et al., 1994). A 421 bp *Sma*I fragment (from position 290 to 711 bp) of the *GATA-3* cDNA (Ko et al., 1991) was subcloned into plasmid pTZ18R, resulting in plasmid pW191a. The antisense RNA probe was transcribed from *Bam*HI linearized pW191a with T7 RNA polymerase. The RNA in situ probe for the mouse *LIF* gene was transcribed from a cDNA fragment spanning from position 3279 to 3721 bp of *LIF* gene (Stahl et al., 1990; Stewart, 1994).

Histology and scanning electron microscopy

For the analysis of inner ears, mice were cardiac-perfused with 4%

paraformaldehyde for tissue sections or 2.5% glutaraldehyde in cacodylate buffer for SEM. Inner ears were rapidly dissected out in fixative at room temperature (RT) and once the bony labyrinths had been removed, they were fixed with shaking for 4 hours at RT and then at 4˚C overnight. The tissue was then decalcified in 10% EDTA at 4˚C for 5 days, then dehydrated in ethanols followed by histoclear (for sections) and paraffin embedding. 7 μm sections were cut and stained with toludine blue and mounted in Permount. For SEM, during dissection the stapedial footplate, round window and the apex of the cochlea were opened to allow fixative penetration. Following washing in PBS, the tissue was osmicated in 1% osmium tetroxide, followed by microdissection in 70% ethanol to remove the utricle, saccule and the utriculosaccular complex, critical point drying and sputter coating essentially as described (Lufkin et al., 1991). The area of macula sensory epithelium for the utricles and saccules of *Hmx-3* wild-type +/+, heterozygotic +/– and homozygotic –/– inner ears was determined by measuring the linear extent of each macula sensory epithelium on every 7 μm section of serial sectioned temporal bones. An eyepiece grid reticule in a Zeiss Axiphot microscope was used to count the number of grid boxes filled with macula sensory epithelium at 62.5× magnification and then the grid box count was converted into an area measurement of sensory epithelium in mm^2 by the following formula:

$$\frac{n \times \text{grid box length} \times \text{section thickness}}{1000 \times \text{magnification factor}} = \text{macula sensory area in } mm^2$$

where n = number of grid boxes, grid box length = 160 μm, section thickness = 7 μm, magnification factor = 62.5.

RESULTS

Hmx3 gene targeting

Genomic clones containing 24 kb surrounding the *Hmx3* gene were isolated from a lambda 129/Sv mouse genomic library by low-stringency screening with a PCR-derived probe corresponding to the human *HMX1* homeobox region (Stadler et al., 1992). Gene targeting constructs were prepared by inserting the neomycin-resistance cassette (*neo*) or the IRES-*lacZ*+neomycin reporter and resistance (*lacZneo*) (Li et al., 1997) cassette into the unique *Xho*I site located in the *Hmx3* homeobox sequence (Fig. 1A). The insertion of either cassette results in the truncation of the Hmx3 protein in the N-terminal portion of the homeodomain (owing to stop codons present in the 5′ portion of each cassette), thus generating a non-functional or null allele. Both constructs were electroporated into embryonic stem (ES) cells and neo-resistant colonies that had undergone a homologous recombination event were identified by Southern blotting. Three positive clones for the $Hmx3^{neo}$ null allele and five positive clones for the $Hmx3^{lacZ}$ null allele were obtained. Positive ES cells were subsequently used to generate germline transmitting chimeras by microinjection of C57BL/6J blastocysts (Fig. 1B). Transmitting chimeras were backcrossed to 129/Sv mice to put the *Hmx3* mutation on a congenic inbred background. To determine that the *Hmx3* gene was functionally disrupted, an RNAse protection assay was performed on embryo RNA using a probe spanning the site where the *neo* cassette had been inserted (Fig. 1A,C). Wild-type embryo RNA protected a fragment of 472 bp, whereas the mutant allele protected bands of 308 bp and 164 bp (Fig. 1C). β-actin was used to control for the quality and quantity of RNA.

Expression from the $Hmx3^{lacZ}$ allele

Expression from the *Hmx3* gene was monitored in $Hmx3^{lacZ}$ heterozygotes by staining for beta-galactosidase activity (Fig. 2). The activity of the inserted *lacZ* transgene displayed an identical pattern of expression relative to the wild-type *Hmx3* RNA distribution obtained by RNA in situ hybridization (Bober et al., 1994; Rinkwitz-Brandt et al., 1995). Earliest expression from the $Hmx3^{lacZ}$ allele was detected at E8.5 in the otic placode and the branchial arch region (Fig. 2A). During the next 24 hours, expression from the $Hmx3^{lacZ}$ allele continues to increase in the otic vesicle and the cleft between the first and second branchial arches (Fig. 2B-F). The expression within the otic vesicle at E9.5 shows an uneven distribution, with greater β-galactosidase activity present in the rostral half of the otic vesicle, which are the group of cells that form the precursor to the vestibular system (Li et al., 1976, 1978). During subsequent stages of embryogenesis, the $Hmx3^{lacZ}$ allele is clearly active in the central and peripheral nervous systems, as well as in the developing inner ear (Fig. 2G-P). Sectioning of E13.5 $Hmx3^{lacZ}$ embryos revealed strong expression in the epithelium of the developing vestibular ducts and no expression in adjacent cochlear epithelium (Fig. 2I-P).

Hmx3 null animals have diminished postnatal viability

Hmx3 heterozygotes were indistinguishable from wild-type animals, and matings between *Hmx3* heterozygotes resulted in viable *Hmx3* null animals. However, among 151 offspring analyzed at 3 weeks of age on a mixed (C57BL/6J × 129/Sv) genetic background only 70% of the expected 1:2:1 Mendelian ratio (+/+:+/–:–/–) of *Hmx3* null animals were present (Table 1), suggesting a decreased fitness associated with the *Hmx3* null genotype. Intermating of *Hmx3* null males with *Hmx3* heterozygote females revealed a similar result among 360 3-week-old offspring, with only 60% of the expected *Hmx3* null animals present at this age. Intermating of *Hmx3* null males with *Hmx3* heterozygote females and the analysis of 283 embryo genotypes from stages E10.5-E18.5 showed the expected Mendelian ratio for heterozygotes and homozygotes (Table 1), suggesting that the decreased number of *Hmx3* null animals at 3 weeks of age was likely resulting from a diminished postnatal viability or selective culling by the mothers.

Circling behavior and inner ear defects in *Hmx3* null animals

By 2 weeks of age, 15% of the *Hmx3* null animals on a mixed genetic background (C57BL/6J × 129/Sv) and 91% of the *Hmx3* null animals on a congenic inbred (129/Sv) background displayed an abnormal energetic circling behavior. The severity of the circling behavior varied between individuals, with the most severely affected mice circling at rates up to 176 revolutions per minute (rpm) for periods of several minutes, interspersed with non-circling periods of feeding, grooming and sleep. The expression of *Hmx3* in the vestibular portion of the developing inner ear suggested a possible connection with the circling behavior. Comparison of the dissected labyrinths from *Hmx3* wild-type, heterozygote and null animals did not reveal any observable external differences in either the formation of the vestibular labyrinth or the cochlear duct (Fig.

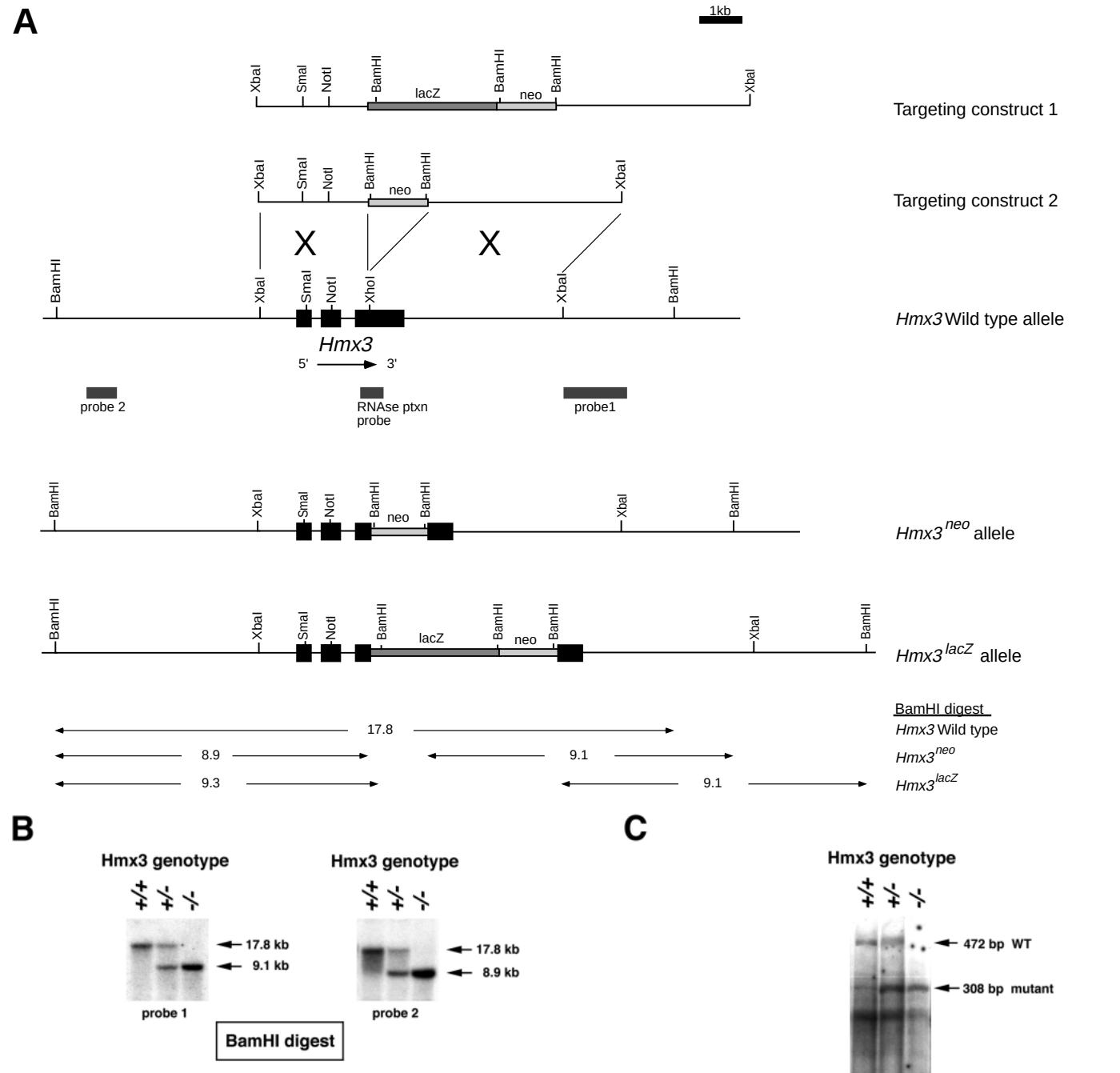

Fig. 1. (A) *Hmx3* wild-type locus, targeting constructs and *Hmx3* mutant alleles. Two targeting constructs were employed to mutate the *Hmx3* gene. Targeting construct 1 has the *lacZ* gene followed by the neomycin-resistance gene (*neo*) inserted into a unique *Xho*I site present in the coding region of the *Hmx3* homeobox. This mutant allele will produce β-galactosidase enzyme and a non-functional truncated *Hmx*3 protein. Targeting construct 2 has just the *neo* gene inserted into the same *Xho*I site. The positions of the *Hmx3* exons are indicated with black rectangles. The two Southern blot probes, which lie outside the targeting constructs, are indicated. The position of the probe used in the RNAse protection analysis (see C) is shown. The sizes and positions of fragments corresponding to the wild-type and mutant alleles after Southern blotting with probes 1 and 2 are shown at the bottom. (B) Southern blot analysis of tailtip DNAs from *Hmx3* wild-type, *Hmx3* heterozygote and *Hmx3* null offspring. Tail DNAs were extracted, digested with *Bam*HI, Southern blotted and probed with either probe 1 or probe 2 (see A). The wild-type *Hmx3 Bam*HI fragment gives a band of 17.8 kb with either probe. The *Hmx3*^{neo} allele produces a band of 9.1 with probe 1 and a band of 8.9 with probe 2. (C) RNAse protection analysis of *Hmx3* RNA expression in *Hmx3* wild-type, *Hmx3* heterozygote and *Hmx3* null offspring. Antisense RNA transcripts derived from a wild-type probe fragments spanning the site used for generating the *Hmx3* mutations were used in a protection assay against RNAs extracted from E11.5 *Hmx3* wild-type, heterozygote and null embryos. The wild-type *Hmx3* transcripts protect a fragment of 472 bp whereas the *Hmx3* mutant transcripts protect two fragments of 308 bp and 164 bp.

3). However, microscopic examination of serial-sectioned labyrinths from *Hmx3* null mice revealed that there were several abnormalities in the vestibular sensory receptors when compared to serial sectioned specimens from wild-type and heterozygote animals. In both the *Hmx3* wild-type and heterozygote vestibular labyrinths the utricle and saccule come into close apposition, but always remain distinct endolymph chambers, communicating only via the utriculosaccular valve (Fig. 4A,C,E). In the vestibular labyrinths of the *Hmx3* null mice, the utricle and the saccule do not remain separate because at the area of close apposition there is a fusion of the endolymphatic chambers of the utricle and saccule forming a common utriculosaccular space (Fig. 4B,D,F). The area of fusion into a common endolymphatic chamber occurs on the underside of the utricular macula creating a common space, which is always associated with a corresponding reduction in the sensory cell area of both maculae. The measurements of the sensory areas of the maculae of the saccule and the utricle of both the *Hmx3* wild-type and heterozygote vestibular labyrinths were essentially identical and therefore these measurements were analyzed as a single unit and are shown as a histogram in Fig. 5. A comparison of the sensory epithelial areas of the utricles and saccules of the *Hmx3* null vestibules to the normal values of the wild-type and heterozygote utricles and saccules shows a highly significant loss of sensory cells from both the macula utriculus ($P<1\times10^{-9}$) and the macula sacculus ($P<1\times10^{-3}$). The *Hmx3* null utricles have lost 35% of their sensory epithelial area and the sensory areas of their saccules have been reduced by 13% (Fig. 5). All of the semicircular ducts were present and appeared normal in the *Hmx3* null inner ears, with the exception of the horizontal semicircular duct, which lacked both a horizontal crista and the associated horizontal ampullary chamber (see Fig. 4). The anterior crista (Fig. 4G,H) and the posterior crista were present and completely normal in the *Hmx3* null vestibular labyrinths. Ultrastructural examination of the utricular sensory epithelium from *Hmx3* wild-type, heterozygote and null animals did not show any differences in either the otoconia or the sensory hair bundles of the maculae (not shown). The expression of *Hmx1*, *Hmx2*, *Hmx3* and zinc-finger transcription factor *GATA3* were examined in the inner ears of wild-type and *Hmx3* null embryos (Fig. 6). *GATA3* was examined in addition to the *Hmx* genes, because it shows specific expression

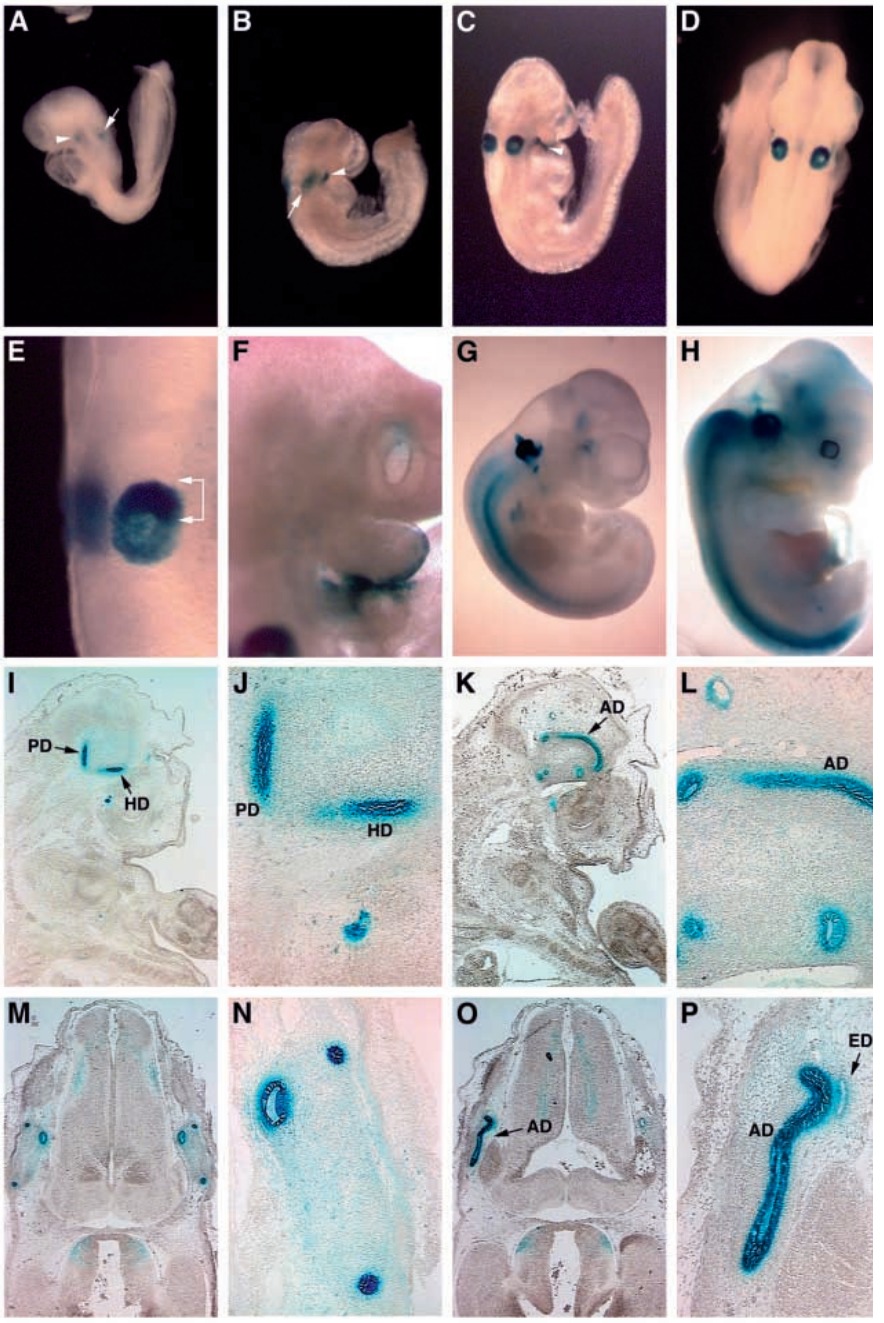

Fig. 2. β-galactosidase expression in *Hmx3*^{lacZ} heterozygotes during embryogenesis. *Hmx3*^{lacZ} heterozygote embryos from stages E8.5-E13.5 were stained for β-galactosidase expression as wholemounts (A-H) and then serial sectioned (I-P). In a manner identical to *Hmx3* RNA expression, E8.5 embryos (A) show the earliest expression of *Hmx3*^{lacZ}, which is seen in the otic placode (arrow) and in the developing branchial arch (arrowhead). E9.0 embryos (B) and E9.5 embryos (C-F) show expression in the otic vesicle (arrow) and in the cleft between the first and second branchial arches (arrowhead in C). The expression within the otic vesicle at E9.5 and later stages shows greater intensity in the rostral half (bracketed in E), which is the tissue that subsequently gives rise to the vestibule. Embryos at later stages (E10.5, G) and (E12.5, H) show qualitatively the same expression as at earlier stages, and additionally now show significant expression in the central and peripheral nervous systems. Sagittal (I-L) or transverse (M-P) sections of E13.5 embryos show the strongest expression of *Hmx3*^{lacZ} in the vestibular portion of the inner ear. Strongest expression is seen within the epithelial portion of the developing vestibule. AD, anterior semicircular duct; ED, endolymphatic duct; HD, horizontal semicircular duct; PD, posterior semicircular duct.

Table 1. Reduced viability of *Hmx3* juveniles

	Genotype		
	+/+	+/–	–/–
A			
3-week pups	39	86	26
Ratio	1.0	2.2	0.7
B			
Embryo stage			
E10.5		43	38
E12.5		45	49
E14.5		29	44
E16.5-E18.5		12	20
Total		129	151
Ratio		1.0	1.2
3-week pups		219	141
Ratio		1.0	0.6

(A) The ratio of observed *Hmx3* null animals at 3 weeks of age derived from heterozygote matings is 30% less than the predicted Mendelian ratio of 1:2:1 for a non-lethal mutation, suggesting that *Hmx3* null homozygotes are less viable than wild-type or *Hmx3* heterozygote animals prior to this stage of development (Chi-square test = 5.16; P=0.076; reject H_0 hypothesis = follow Mendelian 1:2:1 distribution at 92% confidence level). (B) Analysis of the distribution of genotypes from mating *Hmx3* heterozygotes with *Hmx3* null homozygotes revealed no decrease in the percentage of *Hmx3* null embryos prior to birth (E10.5-E18.5; Chi-square test = 1.73; P=0.189; cannot reject H_0 hypothesis = follow Mendelian 1:1 distribution at 90% confidence level) but a 40% reduction in *Hmx3* null animals by 3 weeks of age (Chi-square test= 16.9; $P=3.9\times10^{-5}$; reject H_0 hypothesis = follow Mendelian 1:1 distribution at 99% confidence level).

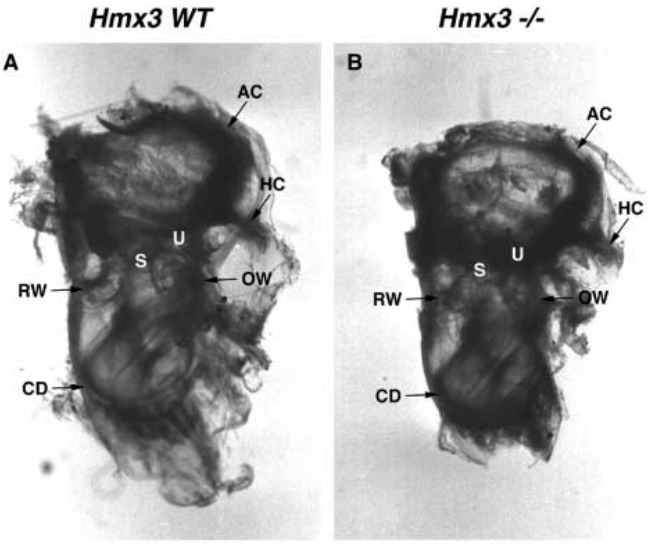

Fig. 3. Macroscopic analysis of *Hmx3* null inner ear morphology. Macrophotographs of whole dissected bony labyrinths from adult wild-type (A) and *Hmx3* null circling (B) animals. Note that there are no grossly observable differences in these bony labyrinths, indicating that the *Hmx3* null phenotype does not involve any severe dysmorphology of inner ear structures. AC, anterior canal; CD, cochlear duct; HC, horizontal canal; OW, oval window; RW, round window; S, saccule; U, utricle.

throughout the otic epithelium during development (George et al., 1994). Significantly, no discernible change in the expression of any of these molecular markers was observed in the *Hmx3* null embryos, suggesting that within the inner ear, neither the *Hmx* genes, nor *GATA3* fall under the direct regulatory control of *Hmx3*. Interestingly, this is in contrast to what was observed for *Hmx* gene expression within the uterus, where significant differences were observed in the *Hmx3* null animals (described below).

Failed pregnancy in *Hmx3* null females

The percentage of *Hmx3* null males that were fertile when tested is very similar to what was found for wild-type males (Table 2). However of 83 *Hmx3* null females tested in monitored matings with wild-type males, 88% were determined to be incapable of carrying out a normal pregnancy or producing litters following repeated independent vaginal pluggings. The remaining 12% of the *Hmx3* null females capable of producing offspring could do so repeatedly, indicating that the penetrance of the infertility characteristic was stable within an individual animal (Table 2). To determine the time point of female infertility, *Hmx3* null females were mated with wild-type males and the plug date monitored. On successive days following plugging, the *Hmx3* null females were killed and the oviducts or uteri were removed and flushed with medium to recover embryonic material (embryos or unfertilized oocytes) that might be present. Flushing of *Hmx3* null females at E0.5-E3.5 resulted in the recovery of viable cleavage-stage embryos at the appropriate gestational age and at normal numbers relative to wild-type animals (Table 3). This indicated that there was apparently normal ovulation, fertilization and preimplantation development taking place in the *Hmx3* null females. When reimplanted into wild-type pseudopregnant animals, the embryos recovered from *Hmx3* null females were able to undergo normal uterine implantation, embryonic development and birth, and were by all criteria indistinguishable from wild-type embryos. In contrast, when wild-type preimplantation-stage embryos isolated from wild-type parents were implanted into pseudopregnant *Hmx3* null females, the *Hmx3* null females failed to undergo a successful implantation and become pregnant (Table 3). Normal embryonic implantation takes place at E4.5, when the blastocyst hatches from the zona pellucida and attaches to the uterine endometrial epithelium. *Hmx3* null females that had been naturally mated with wild-type males were killed at stages E4.5-E12.5 and their uteri examined. In the majority of uteri, no visible decidual swellings or implantation sites were observed, and dissection revealed no stromally implanted embryos (Table 3). When flushed with medium at E5.5, embryos at approximately the hatched blastocyst stage (E4.5-5.5) could be recovered from *Hmx3* null uteri naturally mated with wild-type males. This same flushing procedure is not possible with wild-type females, as the decidual swellings surrounding the embryo implantation sites block any flow of medium through the uterine lumen. Dissection of the uterine wall and deciduum is possible at this and later stages in wild-type females, and this approach revealed, as expected, that most of the implantation sites in wild-type females did contain an embryo embedded in decidual material (Table 3). Taken together, these results suggested that the failure of *Hmx3* null females to support a normal pregnancy was likely occurring around the time of embryo implantation.

Table 2. *Hmx3* null females have reduced post-implantation fertility

Hmx3 genotype	Sex	Mice tested	Individuals capable of successful pregnancy	Percentage of fertile individuals
+/–	F	27	24	89%
–/–	F	83	10	12%
+/–	M	11	11	100%
–/–	M	74	69	93%

27 wild-type and 83 *Hmx3* null females were tested for their ability to become pregnant following three or more independent vaginal pluggings from wild-type males. 88% of the *Hmx3* null females proved incapable of a successful pregnancy following this mating routine. This is in contrast to 11% of the wild-type females who failed to become pregnant under identical conditions. No significant difference was detected in the fertility of the *Hmx3* wild-type and *Hmx3* null males.

Histological and molecular analysis of uteri from *Hmx3* null females

Hmx3 is expressed in the uterus of both non-pregnant and pregnant females (Figs 7 and 8). In non-pregnant uteri, *Hmx3* transcript distribution is localized to the uterine stroma, with highest expression in cells closest to the epithelial layer of the endometrium and expression showing a mediolateral decrease with increasing distance from the uterine lumen. *Hmx3* gene expression changes during pregnancy, showing a marked increase in the myometrial layer, and a decrease to background levels in the uterine stroma. *Hmx1* and *Hmx2* are also expressed in a manner nearly identical to *Hmx3*; however, *Hmx1* shows a relatively lower level of expression in the non-pregnant uterus compared to *Hmx2* or *Hmx3* (Fig. 7).

Several uterine developmental markers that have been shown to play a role in female fertility were examined in wild-type and *Hmx3* null pregnant and nonpregnant uteri. The murine *Wnt* family is homologous to *Drosophila wingless*, and these molecules appear to be involved in cell-cell signaling (McMahon et al., 1992; Nusse and Varmus, 1992). Three *Wnt* genes that are specifically expressed in the adult uterus were examined. *Wnt5A* has been shown to be a critical developmental control gene, and to be specifically expressed in the uterus in a dynamic manner during pregnancy (Huguet et al., 1995; Kuhlman and Niswander, 1997; Pavlova et al., 1994). In wild-type nonpregnant females, *Wnt5A* is expressed in the uterine stroma and very weakly in the endometrial epithelium. In nonpregnant *Hmx3* null females, *Wnt5A* expression is dramatically altered, and is strongly expressed in the endometrial epithelium and at normal levels in the stroma. In wild-type pregnant animals, *Wnt5A* expression is most pronounced in the glandular epithelium embedded in the stroma and in the endometrial epithelium. *Wnt5A* expression is also altered in *Hmx3* null pregnant females with a dramatic overall increase in expression throughout the uterine stroma, with expression increasing in stromal cells located with increasing proximity to the myometrial layer (bracketed, Fig. 7). In addition, in the *Hmx3* null pregnant females *Wnt5A* shows no elevated expression within the endometrial epithelium (Fig. 7).

In addition to expression in the central nervous system,

Table 3. *Hmx3* null females have a block at the peri-implantation stage of pregnancy

Hmx3 genotype ♂ × ♀	Age of embryos	Embryos recovered	Visible implantation sites	Embryos transferred	Foster ♀	Pups born
+/+ × –/–	E0.5	7	-			
+/+ × –/–	E0.5	10	-			
+/+ × –/–	E0.5	6	-	14	+/+	7
+/+ × –/–	E3.5	6	-			
+/+ × –/–	E3.5	4	-			
+/+ × –/–	E3.5	8	-			
+/+ × –/–	E3.5	8	-	22	+/+	13
+/+ × +/+	E3.5	4	-			
+/+ × +/+	E3.5	8	-			
+/+ × +/+	E3.5	2	-			
+/+ × +/+	E3.5	3	-	15	+/+	6
+/+ × +/+	E3.5	6	-			
+/+ × +/+	E3.5	8	-			
+/+ × +/+	E3.5	10	-			
+/+ × +/+	E3.5	9	-			
+/+ × +/+	E3.5	3	-			
+/+ × +/+	E3.5	8	-	44	–/–	0
+/+ × –/–	E5.5	1	0			
+/+ × –/–	E5.5	4	0			
+/+ × –/–	E5.5	0	0			
+/+ × –/–	E5.5	1	0			
–/– × +/+	E5.5	5	5			
–/– × +/+	E5.5	6	8			
–/– × +/+	E5.5	8	10			
–/– × +/+	E5.5	-	8			
+/+ × –/–	E9.5	0	0			
+/+ × –/–	E9.5	0	0			
+/+ × –/–	E9.5	8	10			
+/+ × –/–	E9.5	0	0			
+/+ × –/–	E9.5	0	0			
+/+ × –/–	E9.5	0	0			
+/+ × –/–	E9.5	10	10			
+/+ × –/–	E9.5	0	0			
+/+ × –/–	E11.5	0	0			
+/+ × –/–	E11.5	0	0			
+/+ × –/–	E11.5	0	0			
+/+ × –/–	E11.5	0	0			
+/+ × –/–	E11.5	0	0			
+/+ × –/–	E12.5	0	0			
+/+ × –/–	E12.5	0	0			
+/+ × –/–	E12.5	0	0			
+/+ × –/–	E12.5	0	0			
+/+ × –/–	E12.5	0	0			

The stage of *Hmx3* null female infertility was examined by mating wild-type and *Hmx3* null females with wild-type or *Hmx3* null males. Each line represents the results from an individual male-female mating of the indicated genotype. The dashed line indicates the division between pre- and postimplantation stages of development. Females were killed at the indicated ages, and oviducts or uteri were flushed with medium to collect embryos at preimplantation stages of development or manually dissected at postimplantation stages. Preimplantation embryos were examined microscopically and reimplanted into either wild-type or *Hmx3* null foster females and allowed to develop until birth, or to E18.5 when a cesarean section was performed. Results from the first two groups of females indicate that the *Hmx3* null females produce normal numbers of healthy embryos, which when transferred to wild-type pseudopregnant females give rise to normal offspring. In contrast, when wild-type embryos are transferred to *Hmx3* null pseudopregnant uteri, no embryos survive to term. At postimplantation stage E5.5 of development, unimplanted necrotic embryos can be recovered from the uteri of *Hmx3* null females. At later stages of development, 89% of the *Hmx3* null females show no signs of embryo implantation.

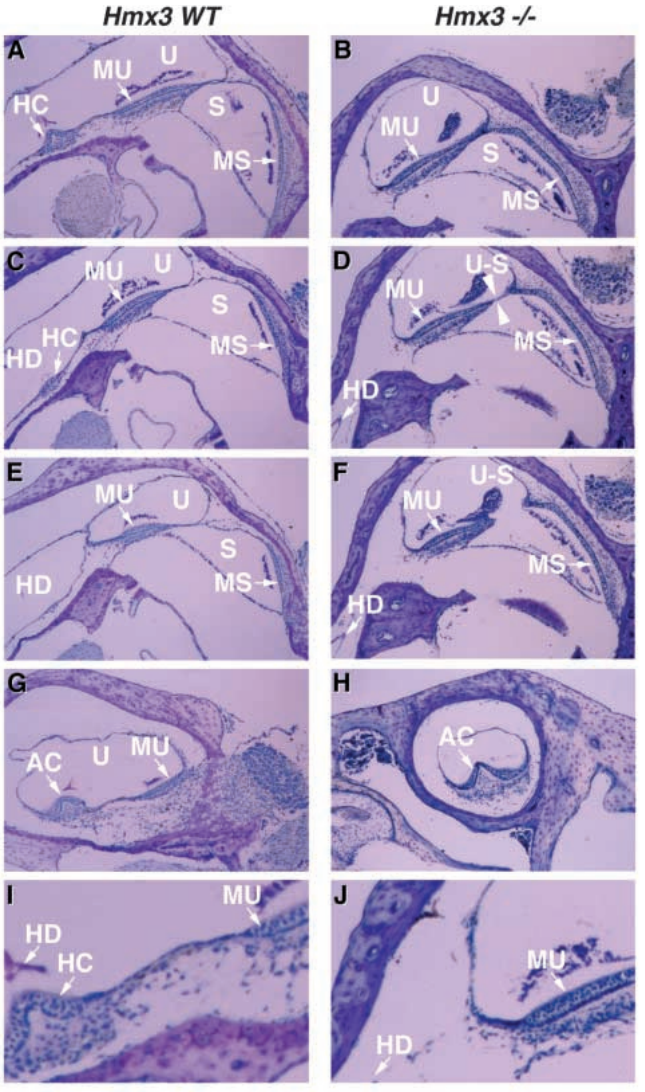

Fig. 4. Histological analysis of inner ear defects in *Hmx3* null mice. Photomicrographs of toludine blue-stained sections of adult temporal bones from wild type (A,C,E,G,I) and *Hmx3* null circling (B,D,F,H,J) inner ears. The sections in A-F represent the area of close apposition of the utricle and saccule. In the wild-type inner ear, there is always a separation of the endolymphatic spaces and maculae of the sensory receptors (see A,C,E). In contrast, serial photomicrographs show a fusion of these two separate sensory receptors into a common utriculosaccular chamber (U-S) with a contiguous endolymphatic space and a reduction in the size of the sensory cell area of the macula utriculus (see B,D,F). Arrowheads in D mark the origin of the fusion. It is also apparent in these serial micrographs that the crista (HC) of the horizontal semicircular duct is not present in the vestibular labyrinth of the *Hmx3* null animal (compare A,C with B,D). This absence of the horizontal crista is presented at higher magnification in (I,J). The cristae of the anterior (AC) and posterior semicircular ducts were present and normal in the vestibular labyrinths of the *Hmx3* null animals. AC, anterior crista; HC, horizontal crista; HD, horizontal semicircular duct; MS, macula sacculus; MU, macula utriculus; S, saccule; U, utricle; U-S, utriculosaccular space.

Wnt7A has previously been shown to be specifically expressed in the adult uterus (Ikegawa et al., 1996). In nonpregnant females, *Wnt7A* is restricted to the luminal epithelium and immediately adjacent stroma, but is absent from the myometrium or glandular epithelium. In pregnant females, *Wnt7A* expression decreases in the luminal epithelium and specifically increases in the myometrium. In *Hmx3* null females, the distribution of *Wnt7A* in nonpregnant females is unaltered, however, in pregnant females; the expression of *Wnt7A* fails to upregulate in the myometrial layer and shows a marked increase in the expression in the luminal epithelium relative to wild-type uteri (Fig. 7). *Wnt4* is expressed in the mesenchyme surrounding the luminal epithelium in nonpregnant wild-type females, and during pregnancy shifts expression to the myometrium and the epithelial glands. In *Hmx3* null females, *Wnt4* expression is absent from the sub-

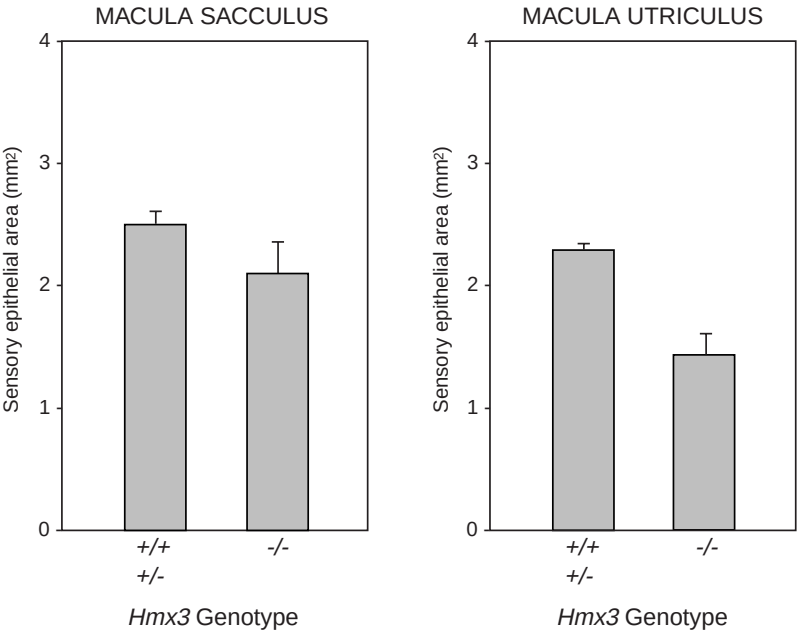

Fig. 5. Quantification of the loss of sensory epithelium in the saccule and utricle. Measurements of the sensory epithelial areas of the utricular and saccular maculae as determined by microscopic measurements of maculae from *Hmx3* wild type (+/+ *n*=2), *Hmx3* heterozygote (+/– *n*=7) and *Hmx3* null (–/– *n*=9) inner ears. Because the area measurements of the maculae of the +/+ and +/– labyrinths were indistinguishable from one another, they were grouped as a single category. A comparison of the mean percentage loss of sensory epithelial area of the *Hmx3* null to the *Hmx3* wild type of the maculae of the utricle showed a highly significant ($P<1\times10^{-9}$) loss of 35% and for the saccule a highly significant ($P<1\times10^{-3}$) loss of 13% of the sensory receptor area.

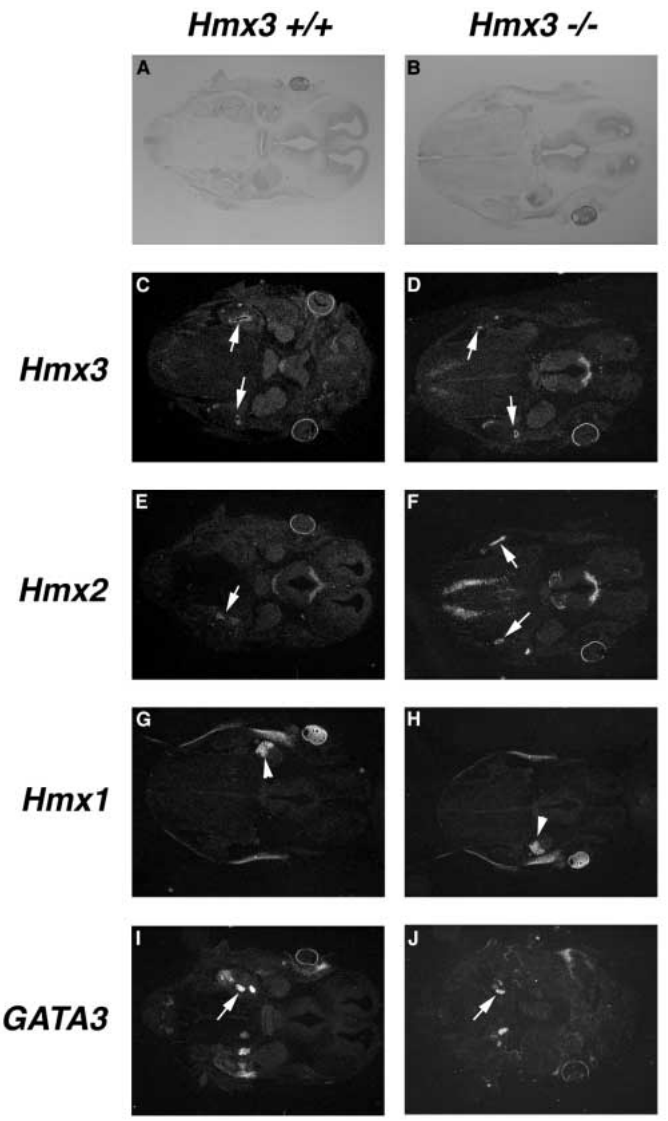

Fig. 6. RNA in situ analysis of gene expression in the inner ear of wild-type and *Hmx3* null animals. Transverse sections through the heads of E14.5 embryos are presented. (A,B) lightfield and (C-J) darkfield. The RNA in situ probe employed (*Hmx3*, *Hmx2*, *Hmx1* and *GATA3*) is shown at the left. The *Hmx3* genotype of the embryos is shown at the top of each column. No significant differences were observed in RNA distribution in the inner ear between *Hmx3* wild-type and *Hmx3* null embryos. Arrows (C,D,E,F,I,J) indicate expression in the semicircular ducts. Arrowhead in (G,H) shows expression in cranial ganglia.

luminal mesenchyme, but is instead expressed specifically within the endometrial epithelium. Furthermore, in pregnant *Hmx3* null females, the expression of *Wnt4* is no longer detected (Fig. 8).

Cytokine leukemia inhibitory factor (LIF) is a maternal product that is absolutely required in the uterus for proper embryo implantation (Stewart et al., 1992). LIF is expressed at low level in the nonpregnant uterus, but at the time of embryo implantation, the glandular epithelium shows a burst of LIF expression (Bhatt et al., 1991; Shen and Leder, 1992). The expression of LIF in nonpregnant *Hmx3* null females appears unaltered. However, in pregnant *Hmx3* null females, LIF fails to show any increase in expression in the glandular epithelium, or in any other uterine tissue (Fig. 8). Myosin is a muscle-specific marker that is specifically expressed in the myometrial layer of the uterus. The myometrium is composed of two layers: an inner layer of circular smooth muscle and an outer layer of longitudinal smooth muscle. Myosin is equally expressed in the two myometrial layers. No change in myosin expression was observed in the *Hmx3* null uteri, in either pregnant or nonpregnant females, indicating there was no gross developmental alteration of the myometrial layer. Likewise, histological examination of the *Hmx3* null uteri revealed no gross alterations of the luminal epithelium, stroma or epithelial glands (Fig. 8).

DISCUSSION

A role for *Hmx3* in vestibular sensory organ specification

The inner ear originates from the otic placode, which is derived from a thickened area of surface ectoderm adjacent to the hindbrain. During embryonic development, the otic placode invaginates to form a cup-like structure, which eventually pinches closed to form the otic vesicle or otocyst. Transplantation experiments, in vitro culturing and genetic studies have determined that signals emanating from the rhombencephalon are critical for the proper development of the otocyst (Van De Water and Represa, 1991). Although the precise signals involved in otocyst formation are unclear, it is likely that members of the FGF cell-cell signaling family (*Fgf3*) play some role in this process (reviewed in (Corey and Breakefield, 1994; Fekete, 1996). During subsequent development, the otocyst undergoes a series of complex morphological changes and cytodifferentiation to give rise to the mature components of the inner ear, which include: three semicircular ducts oriented perpendicular to one another, and associated sensory regions (cristae), which sense angular acceleration; a saccule and utricle and associated sensory regions (maculae), which sense gravity and linear acceleration; and a coiled cochlea, which senses auditory stimuli.

During development, *Hmx3* is first expressed in E8.5 embryos in the otic placode and the branchial arches, thus making *Hmx3* one of the earliest transcription factors to be expressed in the inner ear. During subsequent embryogenesis, *Hmx3* becomes restricted to the dorsorostral portion of the otic vesicle and eventually to the epithelium of the developing vestibular apparatus. The extensive expression of *Hmx3* throughout the vestibular epithelium might suggest possible roles in morphogenesis of the inner ear, or in providing competence for particular vestibular cell fates. In this study we have analyzed the unique genetic role of the *Hmx3* gene during embryonic development and adult life. *Hmx3* lies about 8 kb away from *Hmx2*, and the striking similarity in their expression patterns and in the sequence of their homeodomains, as well as their close proximity on the chromosome, raises the possibility that *Hmx2* and *Hmx3* may share common regulatory elements and have overlapping developmental functions. To avoid deleting any common regulatory elements, the *neo* gene was inserted into the *Hmx3* coding sequence. At the same time, the relatively weak GT1-2 enhancer (Lufkin et al., 1991) was

used to drive *neo* expression in order to minimize the possibility of enhancer/promoter effects on *Hmx2* and potentially other neighboring genes, a problem that has been previously described for the PGK and other promoters (Olson et al., 1996; Rijli et al., 1994). The most striking aspects of the *Hmx3* null phenotype are inner ear vestibular defects and female reproductive failure. The presence of inner ear defects is first indicated in *Hmx3* null juveniles, which display a classic shaker/waltzer behavioral phenotype of circling and hyperactivity (Stein and Huber, 1960). Macroscopic analysis of the inner ears of *Hmx3* null mice failed to uncover any significant gross morphological defects, but further histological analysis revealed a fusion of the utricle and saccule into a common utriculosaccular space, a reduction in the size of the sensory regions (maculae) of both the utricle and saccule, and a complete loss of the sensory region (crista) and associated chamber of the horizontal semicircular duct. These defects alone are sufficient to explain the circling behavioral phenotype of the *Hmx3* null mice.

Three other homeobox-containing genes (*Hoxa-1*, *Otx1* and *Brn3.1*) have previously been shown to affect embryonic development of the vestibule. In *Hoxa-1* null mice the entire endolymphatic labyrinth fails to undergo normal morphogenesis, resulting in complete disruption of the vestibular and cochlear components (Chisaka et al., 1992; Lufkin et al., 1991). The effect of *Hoxa-1* on inner ear development appears to be indirect, as it is never expressed in the otocyst, but rather in the rhombencephalon adjacent to the otocyst. The primary defect in *Hoxa-1* null mice appears to be the deletion of the hindbrain rhombomeres, which normally lie in close apposition to the developing otocyst (Carpenter et al., 1993; Mark et al., 1993), likely resulting in faulty hindbrain-otocyst signaling. Interestingly, apparently normal epithelial thickenings corresponding to cristae and maculae were observed in the *Hoxa-1* inner ears, suggesting that while the overall morphogenesis was disrupted, certain aspects of cellular differentiation remained intact. In comparison, *Otx1* null mice showed complete loss of just the horizontal semicircular duct, with no observed changes in either the anterior or posterior semicircular ducts (Acampora et al., 1996). The *Brn3.1* gene is uniquely expressed in cochlear and vestibular hair cells of the inner ear. *Brn3.1* null mice display a shaker/waltzer behavioral phenotype of circling and hyperactivity and are also completely deaf (Erkman et al., 1996). The histological analysis of the inner ears of *Brn3.1* null mice revealed apparently normal morphogenesis, but a complete failure of hair cell differentiation. Additionally many of the supporting cell populations were absent in the *Brn3.1* null mice, although this is likely a secondary effect of the failed hair cell differentiation. Unlike the *Brn3.1* mutant animals, *Hmx3* null mice show no overt defects in hearing ability nor display any morphological or histological abnormalities of the cochlea. Together with its expression pattern in the dorsal otocyst, it appears that *Hmx3* specifically functions in the development of sensory epithelia of the

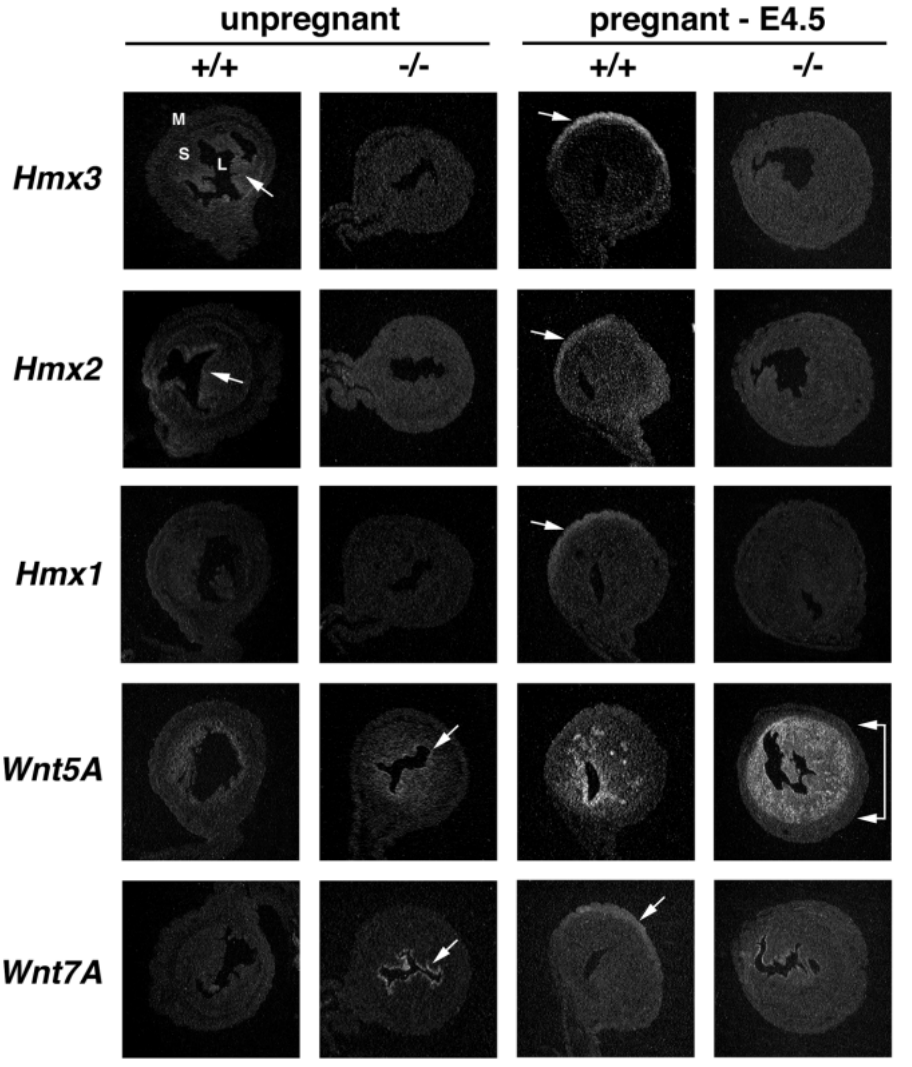

Fig. 7. RNA in situ analysis of altered gene expression in the uteri of *Hmx3* null animals. Transverse sections of uteri in dark field view are presented. The genotype of the female is shown at the top of each column, and whether the female was nonpregnant or pregnant (4.5 days post-coitus) is indicated. The RNA in situ probe employed is shown at the far left of each row. *Hmx3* and *Hmx2* are expressed in the stroma in wild-type nonpregnant uteri (arrows) and *Hmx1-Hmx3* are all upregulated in the myometrial layer in wild-type (+/+) pregnant uteri (arrows). The expression of *Hmx1, Hmx2* and *Hmx3* is no longer detectable in the uteri of *Hmx3* null females. *Wnt5A* is expressed in the endometrial epithelium and adjacent stroma in nonpregnant wild-type females and upregulates in the endometrial epithelium and glands during pregnancy. In the *Hmx3* null females, *Wnt5A* fails to upregulate in the endometrial epithelium, but instead shows dramatic upregulation in the stromal layer. *Wnt7A* shows an upregulation in the *Hmx3* null nonpregnant uteri (arrow) and fails to shift expression to the myometrium during pregnancy. L, uterine luminal cavity; M, myometrium; S, uterine stroma (mesometrium).

vestibular labyrinth. Complete loss of the horizontal crista and partial loss of the maculae of the saccule and utricle might suggest a unique function in vestibular sensory cell fate determination. Since no defects were found in the sensory hair bundles of the maculae, it suggests that *Hmx3* may exert its function prior to hair cell differentiation. Since *Hmx3* is expressed at the earliest stages of inner ear development it may, along with other genes, work to define the regions that will have the competence to give rise to different sensory receptors. If this is the case, once the competent region is determined by *Hmx3*, hair cell development seems to proceed in a *Hmx3*-independent manner. Subsequent cell lineage determination of hair cell versus support cell is likely mediated, in part, by evolutionarily conserved molecules involved in cell-cell lateral inhibition (reviewed in Fekete, 1996). In *Hmx3* null mice, no region is apparently competent to give rise to the horizontal crista, resulting in the absence of this sensory organ. However, the other developing sensory regions may be partially compensated for by the function of other genes, since these regions are able to develop into the maculae of the saccule and utricle, with only a partial loss of sensory cells. Lack of a phenotype in the other two semicircular ducts might be interpreted by an overlap in function with *Hmx2*, since it is strongly expressed in these structures. It can be expected that the double knockout of *Hmx2* and *Hmx3* will show a more severe phenotype than either single knockout, since their overlapping expression patterns and highly similar homeodomains suggest they may function either redundantly or synergistically. In contrast, *Hmx1* is unlikely to contribute directly to inner ear development, as it is never expressed in this structure (Yoshiura et al., 1997). The role of *Hmx3* in inner ear development and pregnancy may be a recently acquired developmental function as *Hmx* genes are present in many species (e.g. *Drosophila*) that have no anatomical equivalent to the organs affected in *Hmx3* null animals. On an evolutionary scale, the mammalian inner ear and uterus represent two relatively newly evolved organs, and the role of *Hmx3* in the development of these structures may represent a more recently acquired function relative to the original role of the ancestral *Hmx* gene. All three *Hmx* genes are expressed in an overlapping fashion in the central and peripheral nervous systems, which may portray the ancestral developmental role of this gene family. The absence of a discernible nervous system phenotype in the *Hmx3* null animals may be related to the ancient origin of the nervous system and the inherent functional overlap between gene family members, which is usually associated with genome evolution (Sidow, 1996).

Hmx3 and maternal reproductive defects

Another important aspect of *Hmx3* gene function is its role in female reproduction. Although *Hmx3* null males showed equivalent fertility relative to wild-type and heterozygous males, 88% of the *Hmx3* null females proved incapable of a successful pregnancy despite repeated independent vaginal pluggings from wild-type males. Examination of the time point of pregnancy failure revealed that *Hmx3* null females produce normal oocytes that can be fertilized and undergo normal preimplantation development. When transferred to wild-type pseudopregnant females, preimplantation embryos isolated from *Hmx3* null females developed to term at normal frequencies, indicating that prior to the implantation stage of pregnancy, *Hmx3* null females can support apparently normal embryonic development. At the implantation stage of pregnancy (E4.5-E5.5) embryos were still unattached in the *Hmx3* null uteri and failed to initiate any decidualization reaction. The peri-implantation period is a critical step in normal pregnancy, as the majority of failed pregnancies occur at this stage (Cross et al., 1994). One gene product which is absolutely required for normal embryonic implantation is the cytokine leukemia inhibitory factor (LIF), which shows a burst of expression in the uterine endometrial glands on E4.5. Like the *Hmx3* null animals, female mice lacking the LIF gene produce normal embryos that can be fertilized and undergo normal preimplantation development but fail to implant in the uterus. When transferred to wild-type foster females, embryos from LIF null females undergo normal implantation, gestation and birth (Stewart, 1994; Stewart et al., 1992). In the *Hmx3* null uterus, LIF fails to undergo its burst of expression during implantation. This effect alone might potentially explain the failed pregnancy phenotype of the *Hmx3* null females.

Two other homeobox genes (*Hoxa-10* and *Hoxa-11*) have been shown to play a critical role in female fertility. In *Hoxa-10* null mice, failed pregnancy results, in part, from an anterior homeotic transformation of the proximal portion of the uterus into tissue resembling oviduct (Benson et al., 1996; Satokata et al., 1995). The anterior transformation is not the only critical factor, however, because implantation of wild-type embryos into the morphologically normal region of the *Hoxa-10* null uterus still resulted in a failed pregnancy, suggesting that other factors important for normal embryonic support are under the control of *Hoxa-10*. Interestingly, the expression of LIF was unchanged in *Hoxa-10* mice, suggesting that some mechanism other than the LIF-mediated cascade was being perturbed. The effect on maternal reproductive failure in *Hoxa-11* null mice was different from *Hoxa-10*. In *Hoxa-11* null females development of stromal, decidual and glandular cells was deficient at early gestational ages (Gendron et al., 1997; Small and Potter, 1993). Furthermore, the *Hoxa-11* null uteri were unresponsive following pseudopregnancy to steroid-induced uterine stromal and glandular cell proliferation and to oil-induced stromal decidualization. Additionally, the *Hoxa-11* null females, like the *Hmx3* null females, fail to show a burst of LIF expression at the time of implantation.

The expression of *Hmx3* in the uterus during pregnancy is dynamic. In nonpregnant females, *Hmx3* is expressed at low levels in the uterine stroma with higher levels closer to the epithelial lumen. During pregnancy *Hmx3* shows a shift to the uterine myometrial layer accompanied by a dramatic upregulation of expression. This upregulation in the myometrium is also observed for both *Hmx1* and *Hmx2*. The significance of the shift of *Hmx3* expression from the stroma to the myometrium is currently unknown, but the genetic analysis performed here demonstrates that the expression of a functional *Hmx3* gene is definitely required for normal implantation. Interestingly, although *Hmx1*, *Hmx2* and *Hmx3* are no longer expressed in the *Hmx3* null myometrial layer, there was no obvious change in the expression of the myometrial smooth muscle marker myosin, indicating that the myosin is likely to fall into a regulatory cascade independent of the *Hmx* genes. The fact that the levels of expression of *Hmx1* and *Hmx2* were both downregulated in the uteri of *Hmx3* null uteri suggest a possible cross or autoregulatory role for the

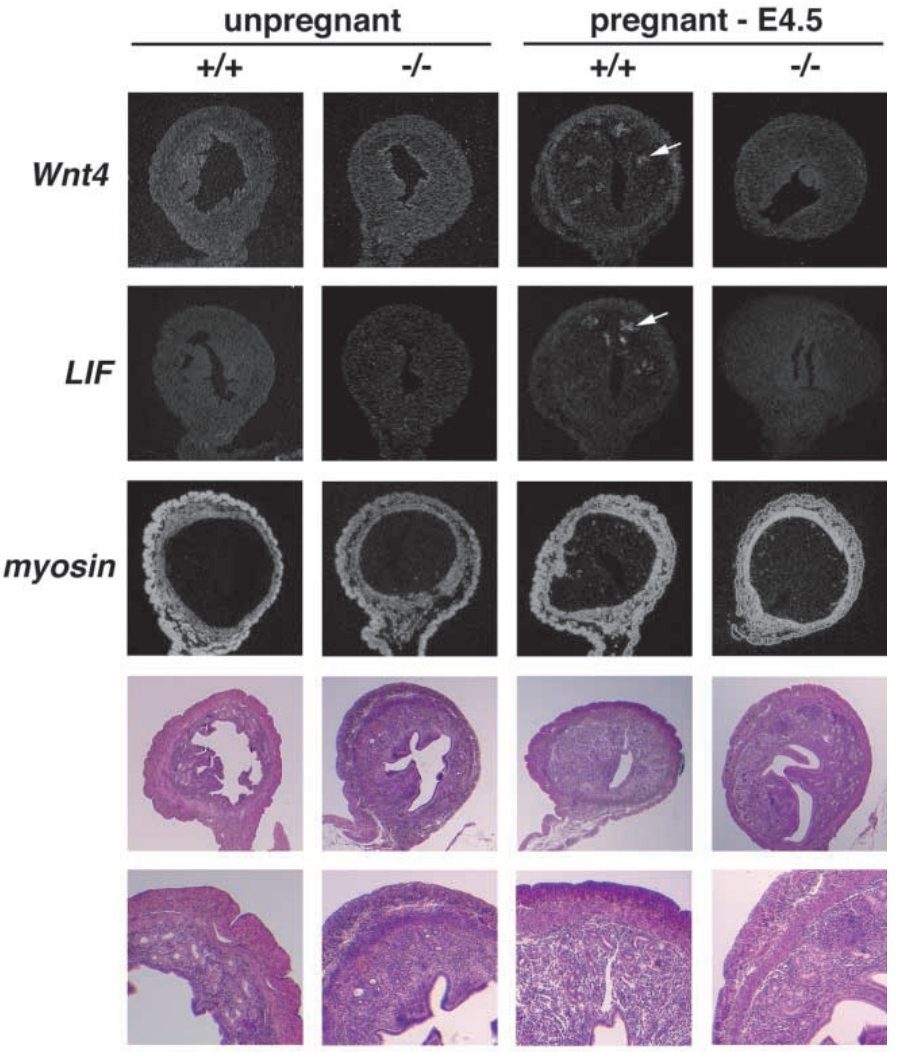

Fig. 8. Histological and molecular analysis of uterine defects in Hmx3 null animals. (Top) Transverse sections of uteri in dark field view are presented. The genotype of the female is shown at the top of each column, and pregnancy status: nonpregnant or pregnant (4.5 days post-coitus) is indicated. The RNA in situ probe employed is shown at the far left of each row. (Bottom) Hematoxylin and eosin-stained sections. Low power view (above) and high power view (below). In wild-type animals, both *Wnt4* and *LIF* are strongly upregulated in E4.5 glandular epithelium (arrows). In *Hmx3* null females, no upregulation of either *Wnt4* or *LIF* is detected. The expression of myosin is unaffected in the *Hmx3* null females. *Hmx3* null females show an apparently normal uterine histology and the epithelial glands appear indistinguishable from wild type.

Hmx genes in the uterus. Cross-regulation and autoregulation of homeobox genes has been well characterized, particularly in the case of the *Hox* homeobox genes (reviewed in (Lufkin, 1997).

Although there were no obvious histological abnormalities in the *Hmx3* null uteri, analysis at the molecular level revealed significant perturbations in gene expression. Three members of the *Wnt* gene family were examined and all showed alterations in their expression patterns. *Wnt5A* is normally upregulated in the endometrial epithelium and the epithelium of the deep glands in wild-type pregnant females. In contrast, in *Hmx3* null pregnant females, *Wnt5A* is no longer upregulated in the endometrial epithelium or the epithelium of the deep glands, but rather shows a widespread activation throughout all the cells of the uterine stroma. Both *Wnt4* and *Wnt7A* normally show an upregulation in wild-type pregnant uteri; however in *Hmx3* null uteri, both genes fail to be activated. Taken together with the results of LIF, *Hmx1* and *Hmx2*, we can conclude that the normal regulatory cascade of gene expression in the uterus has been substantially altered by the loss of the *Hmx3* gene product.

In summary, the *Hmx3* gene plays an important role in murine vestibular sensory organ development and maternal reproduction. To further understand the function of *Hmx3* and the other *Hmx* genes, in addition to *loss-of-function* alleles, equally insightful information will likely be provided from *gain-of-function* studies. Additionally, continued investigation of the role of the *Hmx* genes in other species will only enhance our understanding of the conserved developmental role of this gene family.

We would like to Scott Stadler, Koh-ichiro Yoshiura and Jeff Murray for providing the human and mouse *HMX1* clones and for stimulating discussions, David Sassoon for comments on the manuscript and providing in situ probes, Doug Engel, Colin Stewart and Andy McMahon for RNA in situ probes and Maria Nikolova for technical assistance. This work was supported in part by a grant from the NIH (T. L.) and the Hearing Research Fund of the Montefiore Medical Center (T. R. V.).

REFERENCES

Acampora, D., Mazan, S., Avantaggiato, V., Barone, P., Tuorto, F., Lallemand, Y., Brulet, P., and Simeone, A. (1996). Epilepsy and brain abnormalities in mice lacking the *Otx1* gene. *Nature Genetics* **14**, 218-222.

Benson, G. V., Lim, H. J., Paria, B. C., Satokata, I., Dey, S. K. and Maas, R. L. (1996). Mechanisms of reduced fertility in *Hoxa-10* mutant mice: uterine homeosis and loss of maternal *Hoxa-10* expression. *Development* **122**, 2687-2696.

Bhatt, H., Brunet, L. J. and Stewart, C. L. (1991). Uterine expression of leukemia inhibitory factor coincides with the onset of blastocyst implantation. *Proc. Nat. Acad. Sci. USA* **88**, 11408-12.

Bober, E., Baum, C., Braun, T. and Arnold, H. H. (1994). A novel *NK*-related mouse homeobox gene: expression in central and peripheral nervous structures during embryonic development. *Dev. Biol.* **162**, 288-303.

Carpenter, E. M., Goddard, J. M., Chisaka, O., Manley, N. R. and Capecchi, M. R. (1993). Loss of *Hox-A1 (Hox-1.6)* function results in the reorganization of the murine hindbrain. *Development* **118**, 1063-1075.

Chisaka, O., Musci, T. S. and Capecchi, M. R. (1992). Developmental defects of the ear, cranial nerves and hindbrain resulting from targeted disruption of the mouse homeobox gene *Hox-1.6*. *Nature* **355**, 516-520.

Chomczynski, P. and Sacchi, N. (1987). Single-step method of RNA isolation by acid guanidinium thiocyanate-phenol-chloroform extraction. *Anal. Biochem.* **162**, 156-159.

Corey, D. P. and Breakefield, X. O. (1994). Transcription factors in inner ear development. *Proc. Nat. Acad. Sci. USA* **91**, 433-436.

Cross, J. C., Werb, Z. and Fisher, S. J. (1994). Implantation and the placenta: key pieces of the development puzzle. *Science* **266**, 1508-1518.

Deitcher, D. L., Fekete, D. M. and Cepko, C. L. (1994). Asymmetric expression of a novel homeobox gene in vertebrate sensory organs. *J. Neurosci.* **14**, 486-498.

Erkman, L., McEvilly, R. J., Luo, L., Ryan, A. K., Hooshmand, F., O'Connell, S. M., Keithley, E. M., Rapaport, D. H., Ryan, A. F. and Rosenfeld, M. G. (1996). Role of transcription factors Brn-3.1 and Brn-3.2 in auditory and visual system development. *Nature* **381**, 603-606.

Fekete, D. M. (1996). Cell fate specification in the inner ear. *Curr. Opin. Neurobiol.* **6**, 533-541.

Frasch, M., Chen, X. and Lufkin, T. (1995). Evolutionary-conserved enhancers direct region-specific expression of the murine *Hoxa-1* and *Hoxa-2* loci in both mice and *Drosophila*. *Development* **121**, 957-974.

Gavin, B. J., McMahon, J. A. and McMahon, A. P. (1990). Expresssion of multiple novel *Wnt-1/int-1*-related genes during fetal and adult mouse development. *Genes Dev.* **4**, 2319-2332.

Gendron, R. L., Paradis, H., Hsieh-Li, H. M., Lee, D. W., Potter, S. S. and Markoff, E. (1997). Abnormal uterine stromal and glandular function associated with maternal reproductive defects in *Hoxa-11* null mice. *Biol. Reprod.* **56**, 1097-1105.

George, K. M., Leonard, M. W., Roth, M. E., Lieuw, K. H., Kioussis, D., Grosveld, F. and Engel, J. D. (1994). Embryonic expression and cloning of the murine GATA-3 gene. *Development* **120**, 2673-86.

Gossler, A., Doetschman, T., Korn, R., Serfling, E. and Kemler, R. (1986). Transgenesis by means of blastocyst-derived embryonic stem cells lines. *Proc. Nat. Acad. Sci. USA* **83**, 9065-9069.

Huguet, E. L., Smith, K., Bicknell, R. and Harris, A. L. (1995). Regulation of *Wnt5a* mRNA expression in human mammary epithelial cells by cell shape, confluence and hepatocyte growth factor. *J. Biol. Chem.* **270**, 12851-12856.

Ikegawa, S., Kumano, Y., Okui, K., Fujiwara, T., Takahashi, E. and Nakamura, Y. (1996). Isolation, characterization and chromosomal assignment of the human *WNT7A* gene. *Cytogenet. Cell Genet.* **74**, 149-152.

Ko, L. J., Yamamoto, M., Leonard, M. W., George, K. M., Ting, P. and Engel, J. D. (1991). Murine and human T-lymphocyte GATA-3 factors mediate transcription through a cis-regulatory element within the human T-cell receptor delta gene enhancer. *Mol. Cell Biol.* **11**, 2778-2784.

Kuhlman, J. and Niswander, L. (1997). Limb deformity proteins: role in mesodermal induction of the apical ectodermal ridge. *Development* **124**, 133-139.

Li, C. W., Van De Water, T. R. and Ruben, R. J. (1978). The fate mapping of the eleventh and twelfth day mouse otocyst: an in vitro study of the sites of origin of the embryonic inner ear sensory structures. *J. Morphol.* **157**, 249-267.

Li, C. W., Van De Water, T. R. and Ruben, R. J. (1976). In vitro study of fate mapping of the mouse otocyst. *Trans. Am. Acad. Ophthalmol. Otolaryngol.* **82**, 273-280.

Li, X., Wang, W. and Lufkin, T. (1997). Dicistronic *lacZ* and alkaline phosphatase reporter constructs permit simultaneous histological analysis of expression from multiple transgenes. *BioTechniques* **23**, 874-882.

Lufkin, T. (1997). Transcriptional regulation of mammalian *Hox* genes during embryogenesis. *Crit. Rev. Eukar. Gene Exp.* **7**, 193-213.

Lufkin, T., Dierich, A., LeMeur, M., Mark, M. and Chambon, P. (1991). Disruption of the *Hox-1.6* homeobox gene results in defects in a region corresponding to its rostral domain of expression. *Cell* **66**, 1105-1119.

Lufkin, T., Lohnes, D., Mark, M., Dierich, A., Gorry, P., Gaub, M. P., LeMeur, M. and Chambon, P. (1993). High postnatal lethality and testis degeneration in retinoic acid receptor α mutant mice. *Proc. Nat. Acad. Sci. USA* **90**, 7225-7229.

Mark, M., Lufkin, T., Vonesch, J., Ruberte, E., Olivo, J., Dollé, P., Gorry, P., Lumsden, A. and Chambon, P. (1993). Two rhombomeres are altered in *Hoxa-1* mutant mice. *Development* **119**, 319-338.

Martinez, P. and Davidson, E. H. (1997). *SpHmx*, a sea urchin homeobox gene expressed in embryonic pigment cells. *Dev. Biol.* **181**, 213-222.

McMahon, A. P., Gavin, B. J., Parr, B., Bradley, A. and McMahon, J. A. (1992). The *Wnt* family of cell signalling molecules in postimplantation development of the mouse. In *Postimplantation Development in the Mouse* (ed. D. J. Chadwick and J. Marsh), pp. 199-212. Chichester: John Wiley & Sons.

Miano, J. M., Cserjesi, P., Ligon, K. L., Periasamy, M. and Olson, E. N. (1994). Smooth muscle myosin heavy chain exclusively marks the smooth muscle lineage during mouse embryogenesis. *Circ. Res.* **75**, 803-812.

Nagy, A., Gocza, E., Diaz, E. M., Prideaux, V. R., Ivanyi, E., Markkula, M. and Rossant, J. (1990). Embryonic stem cells alone are able to support fetal development in the mouse. *Development* **110**, 815-821.

Nagy, A. and Rossant, J. (1993). Production of completely ES cell-derived fetuses. In *Gene Targeting: A Practical Approach* (ed. A. Joyner), pp. 147-179. Oxford: Oxford University Press.

Nusse, R. and Varmus, H. E. (1992). *Wnt* genes. *Cell* **69**, 1073-1087.

Olson, E. N., Arnold, H. H., Rigby, P. W. and Wold, B. J. (1996). Know your neighbors: three phenotypes in null mutants of the myogenic bHLH gene *MRF4*. *Cell* **85**, 1-4.

Parr, B. A. and McMahon, A. P. (1995). Dorsalizing signal Wnt-7a required for normal polarity of D-V and A-P axes of mouse limb. *Nature* **374**, 350-353.

Pavlova, A., Boutin, E., Cunha, G. and Sassoon, D. (1994). *Msx1 (Hox-7.1)* in the adult mouse uterus: cellular interactions underlying regulation of expression. *Development* **120**, 335-346.

Rijli, F. M., Dolle, P., Fraulob, V., LeMeur, M. and Chambon, P. (1994). Insertion of a targeting construct in a *Hoxd-10* allele can influence the control of *Hoxd-9* expression. *Dev. Dyn.* **201**, 366-377.

Rinkwitz-Brandt, S., Arnold, H. H. and Bober, E. (1996). Regionalized expression of *Nkx5-1*, *Nkx5-2*, *Pax2* and *sek* genes during mouse inner ear development. *Hear. Res.* **99**, 129-138.

Rinkwitz-Brandt, S., Justus, M., Oldenettel, I., Arnold, H. H. and Bober, E. (1995). Distinct temporal expression of mouse *Nkx-5.1* and *Nkx-5.2* homeobox genes during brain and ear development. *Mech. Dev.* **52**, 371-381.

Sanger, F., Nicklen, S. and Coulson, A. R. (1977). DNA sequencing with chain-terminating inhibitors. *Proc. Natl Acad. Sci. USA* **74**, 5463-5467.

Satokata, I., Benson, G. and Maas, R. (1995). Sexually dimorphic sterility phenotypes in *Hoxa10*-deficient mice. *Nature* **374**, 460-463.

Shen, M. M. and Leder, P. (1992). Leukemia inhibitory factor is expressed by the preimplantation uterus and selectively blocks primitive ectoderm formation in vitro. *Proc. Nat. Acad. Sci. USA* **89**, 8240-8244.

Sidow, A. (1996). Gen(om)e duplications in the evolution of vertebrates. *Curr. Opin. Genet. Dev.* **6**, 715-722.

Small, K. M. and Potter, S. S. (1993). Homeotic transformations and limb defects in *Hox A11* mutant mice. *Genes Dev.* **7**, 2318-2328.

Stadler, H. S., Murray, J. C., Leysens, N. J., Goodfellow, P. J. and Solursh, M. (1995). Phylogenetic conservation and physical mapping of members of the *H6* homeobox gene family. *Mammalian Genome* **6**, 383-388.

Stadler, H. S., Padanilam, B. J., Buetow, K., Murray, J. C. and Solursh, M. (1992). Identification and genetic mapping of a homeobox gene to the 4p16.1 region of human chromosome 4. *Proc. Nat. Acad. Sci. USA* **89**, 11579-11583.

Stadler, H. S. and Solursh, M. (1994). Characterization of the homeobox-containing gene *GH6* identifies novel regions of homeobox gene expression in the developing chick embryo. *Dev. Biol.* **161**, 251-262.

Stahl, J., Gearing, D. P., Willson, T. A., Brown, M. A., King, J. A. and Gough, N. M. (1990). Structural organization of the genes for murine and human leukemia inhibitory factor. Evolutionary conservation of coding and non-coding regions. *J. Biol. Chem.* **265**, 8833-8841.

Stark, K., Vainio, S., Vassileva, G. and McMahon, A. P. (1994). Epithelial transformation of metanephric mesenchyme in the developing kidney regulated by *Wnt-4*. *Nature* **372**, 679-683.

Stein, K. F. and Huber, S. A. (1960). Morphology and behavior of waltzer-type mice. *J. Morphol.* **106**, 197-203.

Stewart, C. L. (1994). Leukaemia inhibitory factor and the regulation of pre-implantation development of the mammalian embryo. *Mol. Reprod. Dev.* **39**, 233-238.

Stewart, C. L., Kaspar, P., Brunet, L. J., Bhatt, H., Gadi, I., Kontgen, F. and Abbondanzo, S. J. (1992). Blastocyst implantation depends on maternal expression of leukaemia inhibitory factor. *Nature* **359**, 76-79.

Tribioli, C., Frasch, M. and Lufkin, T. (1997). *Bapx1:* an evolutionary-conserved homologue of the *Drosophila bagpipe* homeobox gene is expressed in splanchnic mesoderm and the embryonic skeleton. *Mech. Dev.* **65**, 145-162.

Van De Water, T. R. and Represa, J. (1991). Tissue interactions and growth factors that control development of the inner ear. Neural tube-otic anlage interaction. *Ann. NY Acad. Sci.* **630**, 116-128.

Wang, G. V. L., Dolecki, G. J., Carlos, R. and Humphreys, T. (1990). Characterization and expression of two sea urchin homeobox sequences. *Dev. Genet.* **11**, 77-87.

Wang, W., Chen, X., Xu, H. and Lufkin, T. (1996). *Msx3:* a novel murine homologue of the *Drosophila msh* homeobox gene restricted to the dorsal embryonic central nervous system. *Mech. Dev.* **58**, 203-215.

Yoshiura, K., Leysens, N. J., Reiter, R. and Murray, J. C. (1997). Cloning, characterization and gene mapping of mouse *Hmx1*, a new homeobox gene. *Mech. Dev.* (in press).